FINAL REPORT

to:

OFFICE of NAVAL RESEARCH
DEPARTMENT of NAVY

Program Manager
Dr. L.T Kabacoff

Contract: N00014-93-0997

"A Study of Basic Mechanisms Involved in the Consolidation of Multphase Nanostructured Materials"

Principal Investigator
Peter R. Strutt

August 15, 1995

Precision Manufacturing Center, U-119
University of Connecticut, Storrs, Conn., 06269

SECURITY CLASSIFICATION OF THIS PAGE (When Data Entered)

REPORT DOCUMENTATION PAGE

READ INSTRUCTIONS BEFORE COMPLETING FORM

1. REPORT NUMBER

2. GOVT ACCESSION NO.

3. RECIPIENT'S CATALOG NUMBER

4. TITLE (and Subtitle)

A Study of Basic Mechanisms Involved in the Consolidation of Multiphase Nanostructured Materials

5. TYPE OF REPORT & PERIOD COVERED
Final Report
7/15/93 to 7/15/94

6. PERFORMING ORG. REPORT NUMBER

7. AUTHOR(s)

P. R. Strutt

8. CONTRACT OR GRANT NUMBER(s)
N00014-93-0997

9. PERFORMING ORGANIZATION NAME AND ADDRESS
Metallurgy Department & Precision Manufacturing Center, University of Connecticut, Storrs, Conn., 06269

10. PROGRAM ELEMENT, PROJECT, TASK AREA & WORK UNIT NUMBERS

11. CONTROLLING OFFICE NAME AND ADDRESS

12. REPORT DATE
August 15, 1995

13. NUMBER OF PAGES
20

14. MONITORING AGENCY NAME & ADDRESS (if different from Controlling Office)
Office of Naval Research
Arlington, VA

15. SECURITY CLASS. (of this report)
Unclassified

15a. DECLASSIFICATION/DOWNGRADING SCHEDULE

16. DISTRIBUTION STATEMENT (of this Report)

DISTRIBUTION STATEMENT A
Approved for public release
Distribution Unlimited

17. DISTRIBUTION STATEMENT (of the abstract entered in Block 20, if different from Report)

18. SUPPLEMENTARY NOTES

19. KEY WORDS (Continue on reverse side if necessary and identify by block number)
Consolidated Nanostructured Materials
Novel nanoprecipitate morphology
Thermal Spraying of nanostructured coatings
High-voltage/ high resolution electron microscopy

20. ABSTRACT (Continue on reverse side if necessary and identify by block number)

Programmatic achievements made under contract N00014-93-0997 include:

(i) demonstrating that nanostructured WC-Co powder can be thermally sprayed to form nanostructured coatings on substrate materials using the High-velocity Oxyfuel method.

(cont.)

DD FORM 1 JAN 73 1473 EDITION OF 1 NOV 65 IS OBSOLETE

SECURITY CLASSIFICATION OF THIS PAGE (When Data Entered)

(ii) showing that the microstructural scale of the deposited n-WC/Co coatings compares with that of bulk consolidated material (200 nm.).

(iii) showing that chemical changes during actual thermal spraying are completely eliminated by using an experimental gun with a high chamber pressure.

(iv). discovering the existence of ultrafine cobalt precipitates in WC nanograins in bulk consolidated n-WC/Co. These nanoprecipites, which result from the intimate mixing of elements at the molecular level, are believed to be important in promoting fracture toughness.

1. Introduction

One programmatic achievement is a demonstration that nanostructured WC-Co (n-WC/Co) powder can be thermally sprayed to form nanostructured coatings on substrate materials. The first step is the reprocessing of chemically synthesized n-WC/Co powder into feedstock for a conventional High-Velocity OxyFuel (HVOF) thermal spray gun. In the process that was developed, the thermal spray powder consists of agglomerated WC/Co nanoparticles, where the individual particles are solid spheres ranging from 10 to 25 microns in diameter.

The HVOF thermal spray method was selected to deposit coatings, since the short residence time in the flame ensures minimal structural and chemical modification during deposition. Analysis of deposited coatings, shows that although some grain coarsening does occur in the HVOF flame, the mean grain size is 200nm. This value compares with that in bulk consolidated n-WC/Co, and interestingly, the use of a grain growth inhibitor, such as VC, is not required.

It was shown that selecting processing conditions that minimize chemical changes in the flame is particularly important for depositing n-WC/Co coatings by the HVOF method. The strong tendency for conversion of WC to W_2C and W phases was particularly apparent in the initial experiments. The situation was significantly improved however, by enveloping the flame within a nitrogen shroud gas. In later work, preliminary tests showed a novel adaptation to be particularly effective in reducing and even eliminating the deleterious chemical conversion of WC.

In addition to studies on thermally sprayed coatings, comparative studies were conducted on bulk consolidated material. The investigation included studying materials produced by consolidation (i) above the eutectic temperature by liquid phase sintering and (ii) below the eutectic temperature by thermomechanical working. In the case of liquid phase sintered material, the study includes examining the influence of a VC additive on morphological features, as well as its effect in inhibiting grain growth. Electron microscope examination of all consolidated materials reveals a dispersion of nanoprecipitates within the WC nanograins of the nanostructured WC-Co cermet. Microdiffraction and analytical studies show that these nanoprecipitates are f.c.c. cobalt. This novel discovery is consistent with the concept that the nanoprecipitates nucleate from cobalt retained within the WC nanograins, which is a consequence of the intimate intermixing of tungsten and cobalt in the original chemical synthesis process.

2. Reprocessing of Nanostructured Powders for Thermal Spraying

Initially, experiments were performed using as-chemically synthesized n-WC/Co powders supplied by Nanodyne Corp. as feed material, since these consist of nanoparticles agglomerated into hollow spherical shells. Typically, the mean diameter of an individual agglomerated particle is 50 microns, which is in the range suitable for HVOF thermal spraying. Although these powders displayed particularly good flow characteristic when feed into the HVOF, they did not produce fully dense coatings. This arose because of the porosity introduced by incomplete flattening of the hollow spherical particles as they impacted upon the substrate. After recognizing this problem a method was developed to convert the as-received Nanodyne powders into material consisting of solid spherical particles.

The sequence of steps required to produce solid spherical particle powders from chemically or physically synthesized n-powders are summarized diagrammatically in Figure 1. The four synthesis methods represented in Figure 1. are (A) solution/precipitation, (B) spray conversion processing and thermal conversion in a fluid or fixed bed reactor, (C) chemical vapor condensation, and (D) thermochemical spraying. As indicated, whatever the source of n-powder, after re-processing the resulting solid particle agglomerates are about 5-25 microns diameter. These particle agglomerates are sprayable in conventional plasma and high velocity oxy/fuel (HVOF) spray guns.

By way of illustration, we will consider the preparation of sprayable n-WC/Co powder agglomerates, starting from chemically synthesized powder purchased from Nanodyne Inc. In the as-synthesized condition, the n-WC/Co powder particles are highly porous and have a characteristic spherical shell morphology, and, therefore, are inherently fragile. Researchers at PMC have shown that such powders can be ultrasonically disintegrated and uniformly dispersed in a liquid medium. Within minutes, the spherical shell particles (typically < 50 microns diameter), can be reduced to sub-micron dimensions to form a viscous slurry. The liquid medium can be water-base or organic-base, depending on the desired characteristics of the spray dried agglomerated powder. In the water-base case, an emulsion of commercially available polyvinyl alcohol (PVA), polyvinylpyrilidone (PVP), carboxymethyl cellulose (CMC), or some other water soluble polymer, is diluted in de-ionized water, and the solution is spray dried in hot air. In the organic-base case, about 10% of

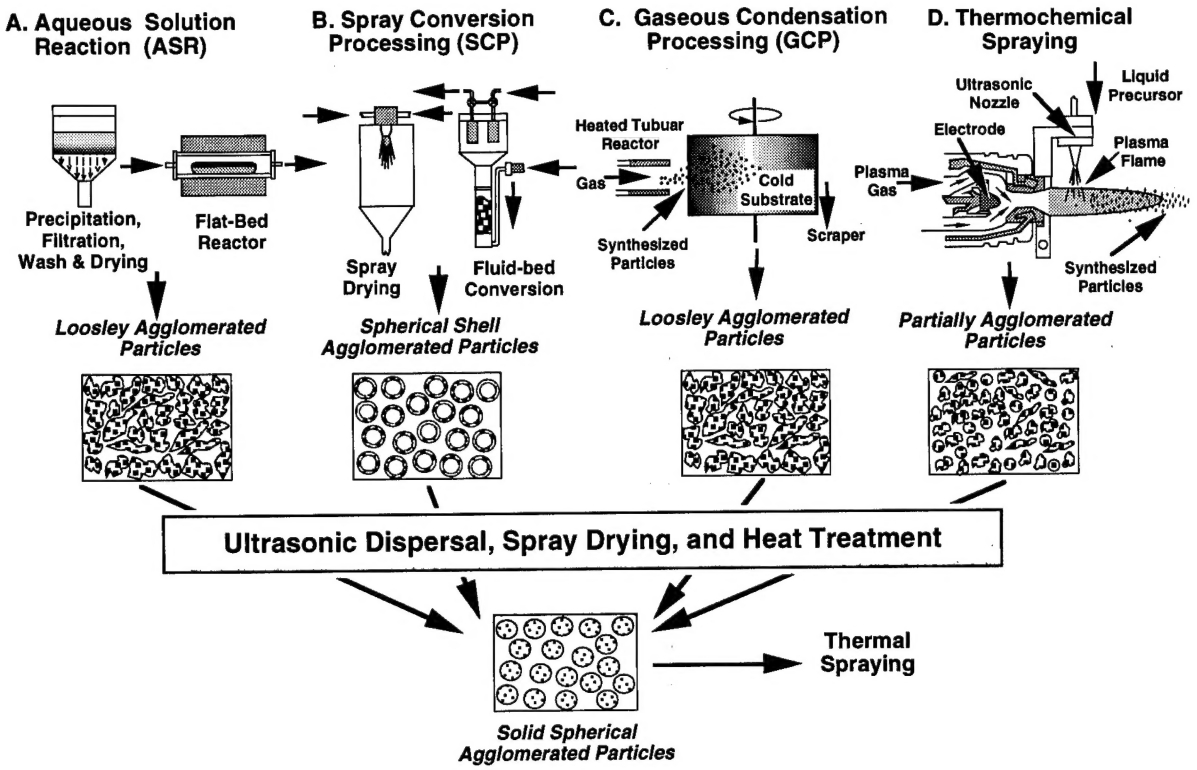

Fig.1 Various powder synthesis methods and the approach for re-processing these into a form suitable for thermal spraying in a conventional powder feed systems.

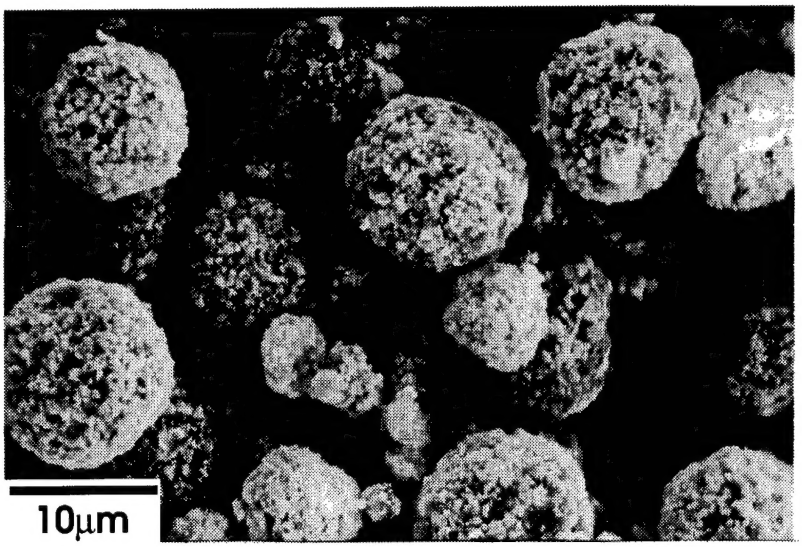

Fig.2 Scanning electron micrograph showing spherical agglomerated nanoparticles of chemically synthesized WC-Co.

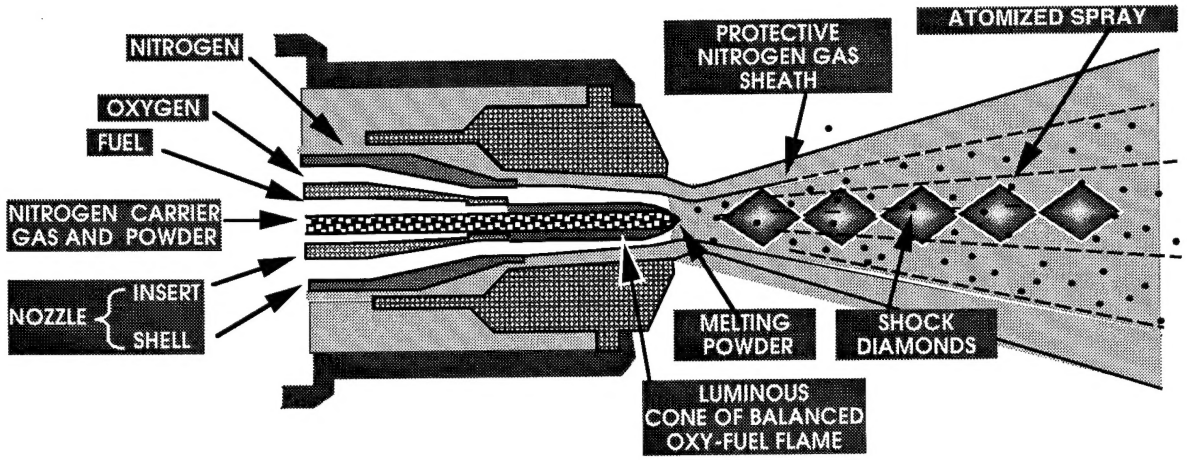

Fig.3 The Metco High-velocity Oxyfuel (HVOF) thermal spray gun, using nitrogen as a protective gas sheath to minimize the chemical reduction of WC carbide particles to W_2C and W. The "shock diamonds" in the flame result from the supersonic gas velocity.

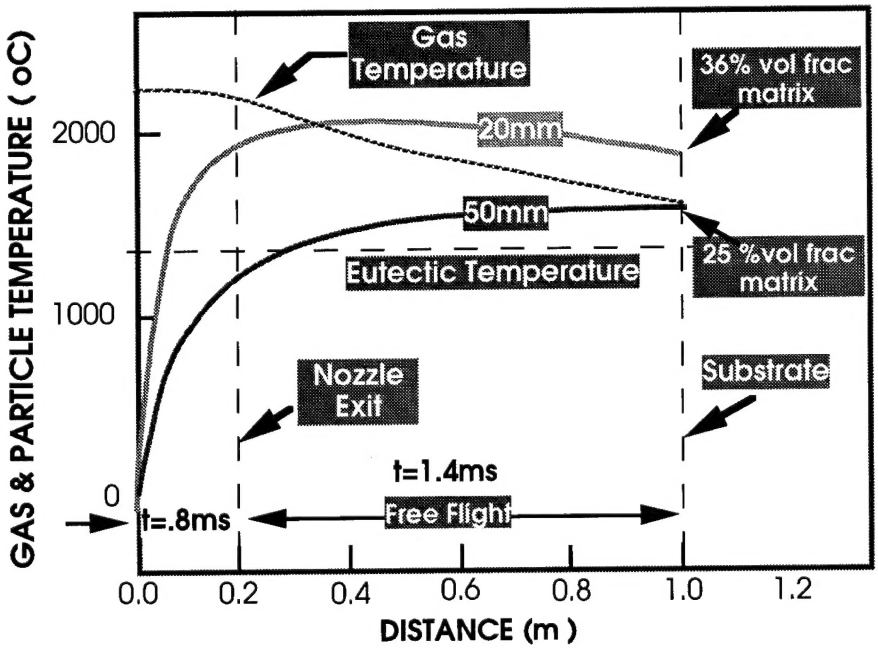

Fig.4 Schematic showing in-flight particle and gas temperature for 20 and 50 μm particle diameters : vol. frac. of matrix due to superheating above the eutectic temperature is shown.

paraffin is dissolved in hexane, pentane or some other organic solvent, and spray dried in hot nitrogen or argon. Water-base solutions are preferred because there is no requirement for the treatment of exhaust gases from the spray drier. The final heat treatment of the spray dried powders is carried out at low temperatures (< 250 C) to expel residual moisture, but leave the organic component as a binder phase.

Figure 2 is an electron micrograph showing particles of a reprocessed powder of nanostructured WC-Co, as is evident the individual particles are spherical with diameters ranging from 10 to 25 microns.

3. HVOF Thermal Spraying of Reprocessed Nanostructured Powders

A schematic diagram of the Metco HVOF gun used to deposit nanostructured coatings is shown in Figure 3. In this deposition process propylene-oxygen combustion produces a flame, where the supersonic combustion gas propels a stream of powder particles injected into the gun. The "shock diamonds" shown in the diagram are shock wave fronts in the supersonic flame. Computer simulation of the HVOF process provides insight into thermal spray deposition of both conventional and n-cermet powders. Figure 4, for example, shows that the high velocity gas stream propels powder particles from the gun nozzle to the substrate surface in a time of 1-2 milliseconds. Following impact, the "mushy" nanostructured particles spread over the surface in about 1 microsecond prior to solidification. Actual solidification is particularly rapid, and occurs in about 0.1 microseconds. From a morphological viewpoint, a feature of Figure 4 is that the WC-Co eutectic temperature is reached in about 1 millisecond. In conventional cermet powder, the large carbide (micron-scale) particles undergo little change in size in this period of time, because of their slow dissolution kinetics. In the nanostructured case, however, carbide dissolution kinetics are particularly rapid, because of the high surface area of contact between the carbide particles and liquid matrix phase. Furthermore, there is a strong tendency for the nanoparticles to agglomerate together to form larger WC grains, as is observed in the consolidation of bulk material.

The present experimental results show that although larger WC grains do form during thermal spraying, a relatively small WC grain size is still maintained. Thus, the grain size as determined from metallurgical sections of deposited material is no more than 200nm., the structure obtained is shown in the electron micrograph in Figure 5. This value is comparable to that in bulk material consolidated by (i) liquid phase sintering of VC-doped

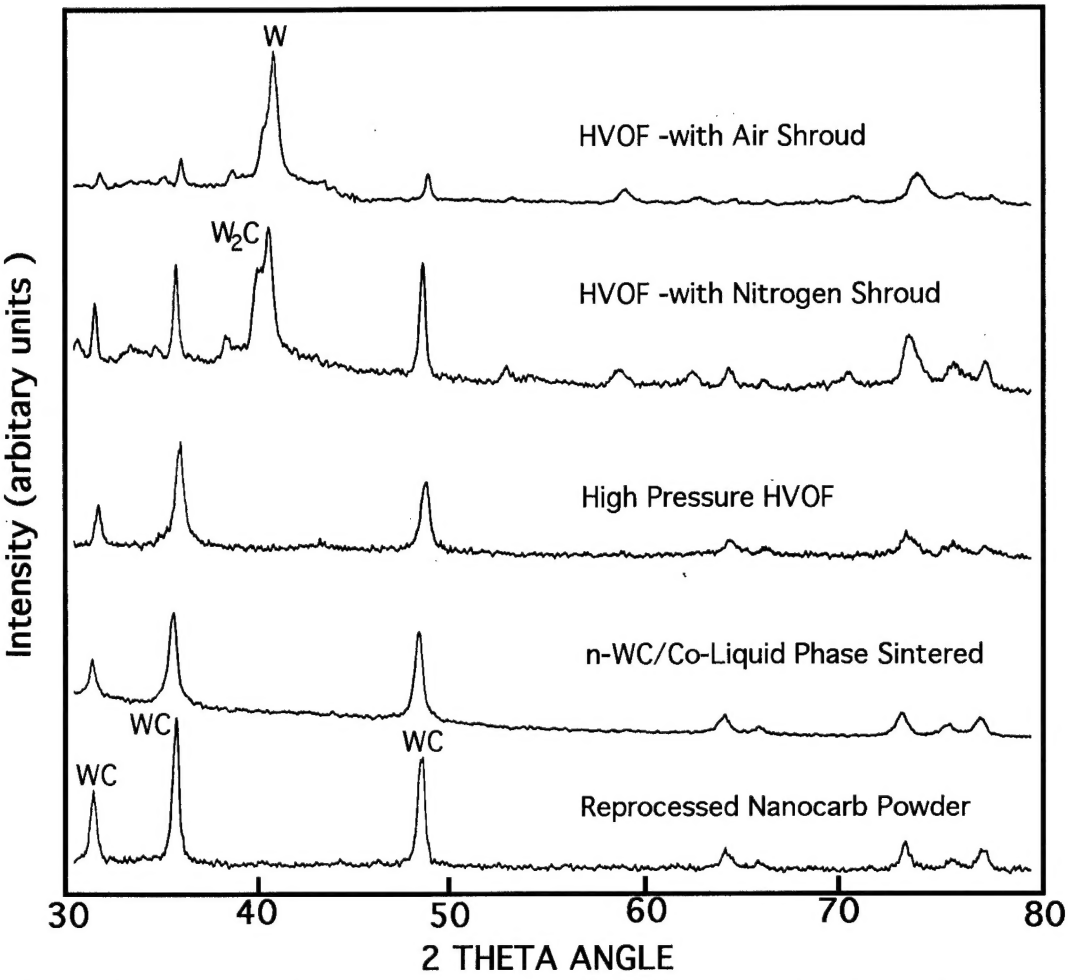

Fig.5 X-ray spectra for nanostructured WC-Co deposited by thermal spray deposition (upper three curves) compared with bulk consolidated material (liquid phase sintered) and thermal spray feed powder (Reprocessed Nanocarb Powder)

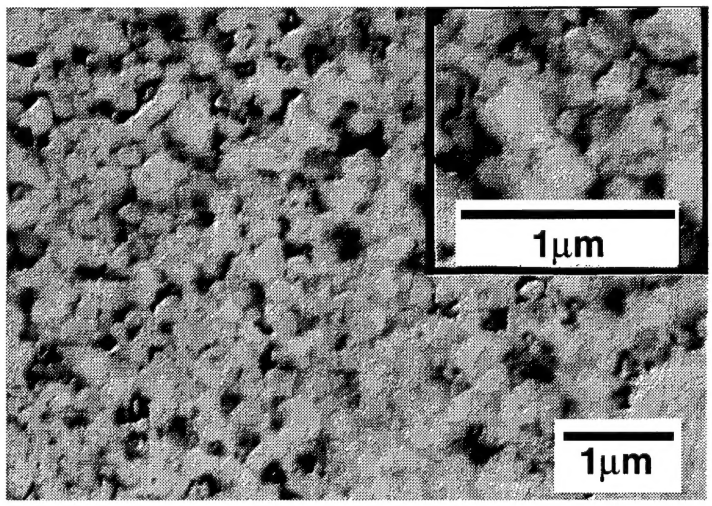

Fig.6 Scanning electron micrograph of thermal sprayed nanostructured WC-Co coating.

n-WC/Co powders and (ii) thermomechanical working below the eutectic temperature.

Although experimental results showed that n-WC/Co material can be successfully deposited without significant WC grain coarsening, it was found that chemical changes occurring in the HVOF flame can be detrimental. Clear evidence of this behavior is provided by X-ray spectra, see Figure 6. Initially, coating deposition was conducted using the Metco gun in its normal mode, where an outer air shroud envelopes the central flame. As shown in the upper spectra in Figure 6. considerable conversion of WC has occurs to produce W_2C and W. Since the detrimental. conversion occurs by oxidative reaction, tests were conducted using a nitrogen shroud gas. As shown by the X-ray spectra, this results in a considerable improvement, since strong WC peaks are now evident.

In later work particularly encouraging results in eliminating the deleterious WC to W_2C and W conversion were obtained using a , novel process adaptation. This involved using the original HVOF gun designed by Browning at a high chamber pressure, by applying an oxygen pressure of 1000 psi. The magnitude of this value is appreciated by noting that the pressure in the Tafa combustion chamber gun is 140 psi, while that in the Metco gun is only 35 psi. The use of a particularly high chamber pressure (1000 psi) achieves (i) a high gas, and hence particle velocity, and (ii) a relatively low gas temperature. The high velocity (i) of the impacting particles results in the deposition of a fully dense coating, and the reduced particle temperature (ii) precludes melting of the Co matrix phase. Thus the deposition process is somewhat analogous to hot working, as employed in the Ceracom bulk consolidation process. In the trail tests using the Browning gun, it should be mentioned that conventional WC/Co powder was used to form the coating, see Figure 7. There were however, two fortuitous benefits in using this material. The first is that the angular shape of the WC grains provides evidence that no melting occurrs during coating deposition. The second is that the relatively high density of small particles (about 300nm diameter) contrasts with that micron sized particles in the feed material, this suggests that particles fragment upon impacting the substrate. The X-spectra for deposited coating of this material, see Figure 5, clearly shows the absence of W_2C and W peaks. As seen in Figure 5,. the spectra is identical to that of the initial powder and consolidated bulk material.

Based upon the experiments performed in the study we conclude that n-WC/Co coatings can be successfully deposited with a grain size comparable with to that in conventionally consolidated material.

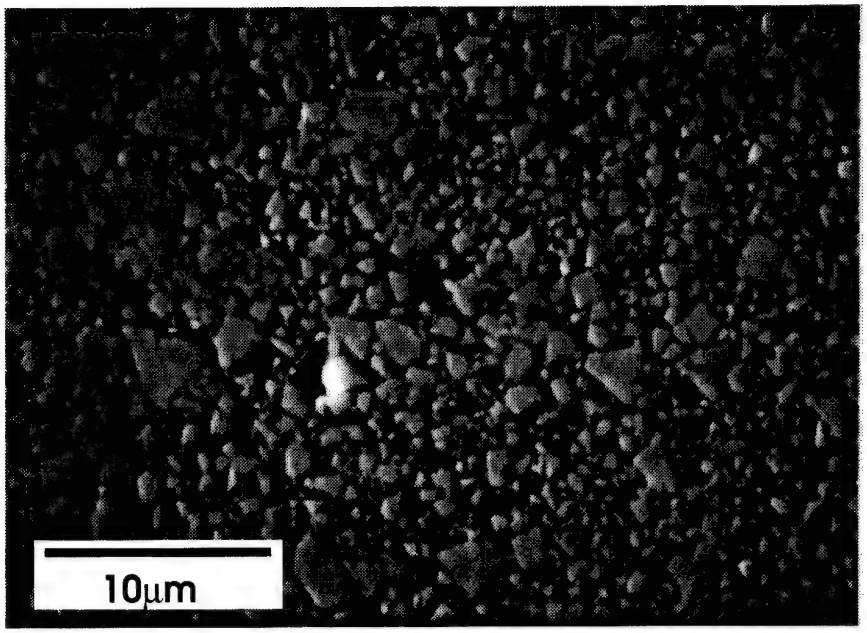

Fig.7 Scanning electron micrograph of WC-Co thermal sprayed coating using a Browning oxyfuel gun operated at an unusually high combusion chamber pressure to produce a high particle velocity and reduced particle temperature. The coating was formed using a conventionally processed powder. The jagged WC particle shape provides evidence that deposition occured without melting.

Also, evidence strongly supports the concept that detectable changes in chemistry can be eliminated by using a high gas velocity gun.

4. Novel Structures in Bulk Consolidated Nanostructured WC-Co

We now report the observation of a novel morphological feature in nanostructured WC-Co synthesized by Aqueous Solution Reaction (ASR) processing, namely the dispersion of ultrafine Co-rich precipitates in WC nanograins. It is proposed that the nucleation of the ultrafine Co-rich precipitates is a consequence of the intimate mixing of the constituent elements a the molecular level.

4.1 *Experimental Techniques and Results*

Nanostructured WC-Co powders produced by Nanodyne Corp., NJ. using the ASR process were consolidated by (i) liquid phase sintering above the eutectic temperature and (ii) hot deformation processing below the eutectic temperature. Materials with compositions of (i) WC-6wt.%Co-0.8wt%VC (ii) WC-6wt%Co (iii) WC-15wt%Co-1.0wt%VC (iv) WC-15wt%Co. were consolidated by Rogers Tool Works[3] by liquid phase sintering at 1400 °C for 1.5 hours. Also, material of WC+6wt.%Co composition was consolidated by Ceracon using hot deformation processing[4] (Ceracon™ process) at temperatures 1200 °C and 1300 °C (i.e. below the ternary eutectic temperature).

The majority of the metallographic specimens were prepared from the as-received material by sectioning with a diamond blade and then polishing. Two samples of WC-6wt.%Co-0.8wt%VC were heat treated at 500 and 700 °C for 8 hours to detect coarsening of the cobalt rich precipitates within the WC nanograins. The samples were heat treated in an quartz tube which had been repeatedly flushed with Argon and then evacuated and sealed. Microhardness measurements were made on the metallographic specimens using a LECO microhardness tester. Electron microscope thin film specimens were prepared by electron discharge machining of 3 mm discs. These were dimpled, prior to perforating the sample by ion beam thinning at 5 kV. The specimens were examined by x-ray diffraction, scanning electron microscopy and transmission electron microscopy Special techniques included high resolution electron microscopy and analytical electron microscopy using JEOL-200 CX, and JEOL-1000 ARM instruments at the National Center for Electron Microscopy (NCEM), Lawrence Berkeley Laboratory (LBL), CA. The specimens on which analytical work was performed were mounted on a cryo-stage and cooled to -150°C. to minimize

thermal drift. A probe size of 100 °A was used to collect the EDAX spectra, as well as micro-diffraction information. All the spectra were acquired to 100,000 total counts to facilitate effective background subtraction and permit quantitative analysis.

Values of the microhardness obtained on the metallographically prepared specimens are shown in Table I. For WC+6wt.% Co material, a particularly high hardness of 2129 VHN is obtained in the liquid phase sintered material containing 0.8 wt%VC as a grain growth inhibitor. This compares with 1732 VHN obtained when there is no VC addition. Interestingly, high VHN values of 2100 and 2200 are obtained in WC+6wt.% Co material when compressive deformation is applied below the eutectic melting point temperature, at 1200 and 1300. Thus, the driving force for WC grain growth is drastically reduced when the cobalt matrix remains solid. It is interesting to note that a reasonably high hardness(1718 VHN) is obtained in liquid phase sintered material containing 1% wt.VC, when the Co content is as high as 15%.

TABLE I

Binder content + %VC	VHN	Consolidation Method
6wt.% Co + 0.8 wt%VC	2129	Liquid Phase Sintering
6% wt.Co	1732	" " "
15% wt.Co + 1% wtVC	1718	" " "
15%wt.Co	1160	" " "
6% wt.Co (compressed at 1200°C)	2100	Hot Mechanical Working
6% wt.Co (compressed at 1300°C)	2210	" " "

Electron microscope observations of the nanostructured WC-Co and WC-Co-VC materials listed in Table I were studied by observing 12 thin film specimens. The general morphological features observed in these specimens are illustrated in Fig.8. Figs.8a and b compare the structure of undoped and VC doped WC-15wt.%Co materials, consolidated by liquid phase sintering using identical processing conditions. The effectiveness of the VC in inhibiting WC phase grain growth is seen by noting that the microstructural scale of the undoped material, in Fig.8(a) is five to ten times that of the VC doped material in Fig.8b. Comparative morphologies of WC-6wt.% Co material consolidated by liquid phase sintering at 1400°C, and

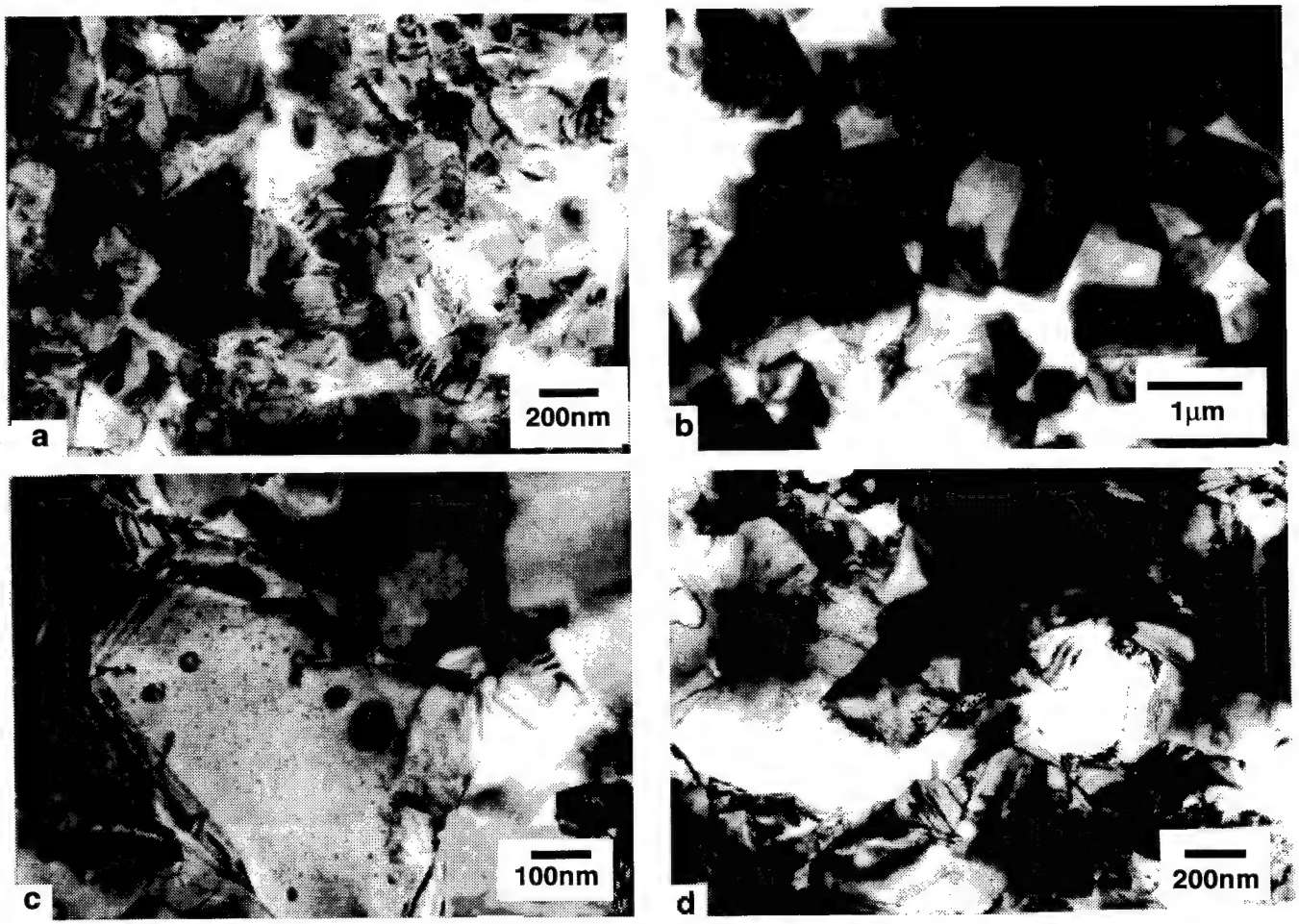

Fig. 8 Transmission electron micrographs of nanostructured (a) WC-15wt%Co, (b) WC-15wt%Co-1wt%VC, and (c) WC- 6wt%Co-0.8wt%VC, consolidated at 1400^{o}C by liquid phase sintering, also (d) WC-6wt%Co, consolidated below the eutectic temperature by thermomechanical working.

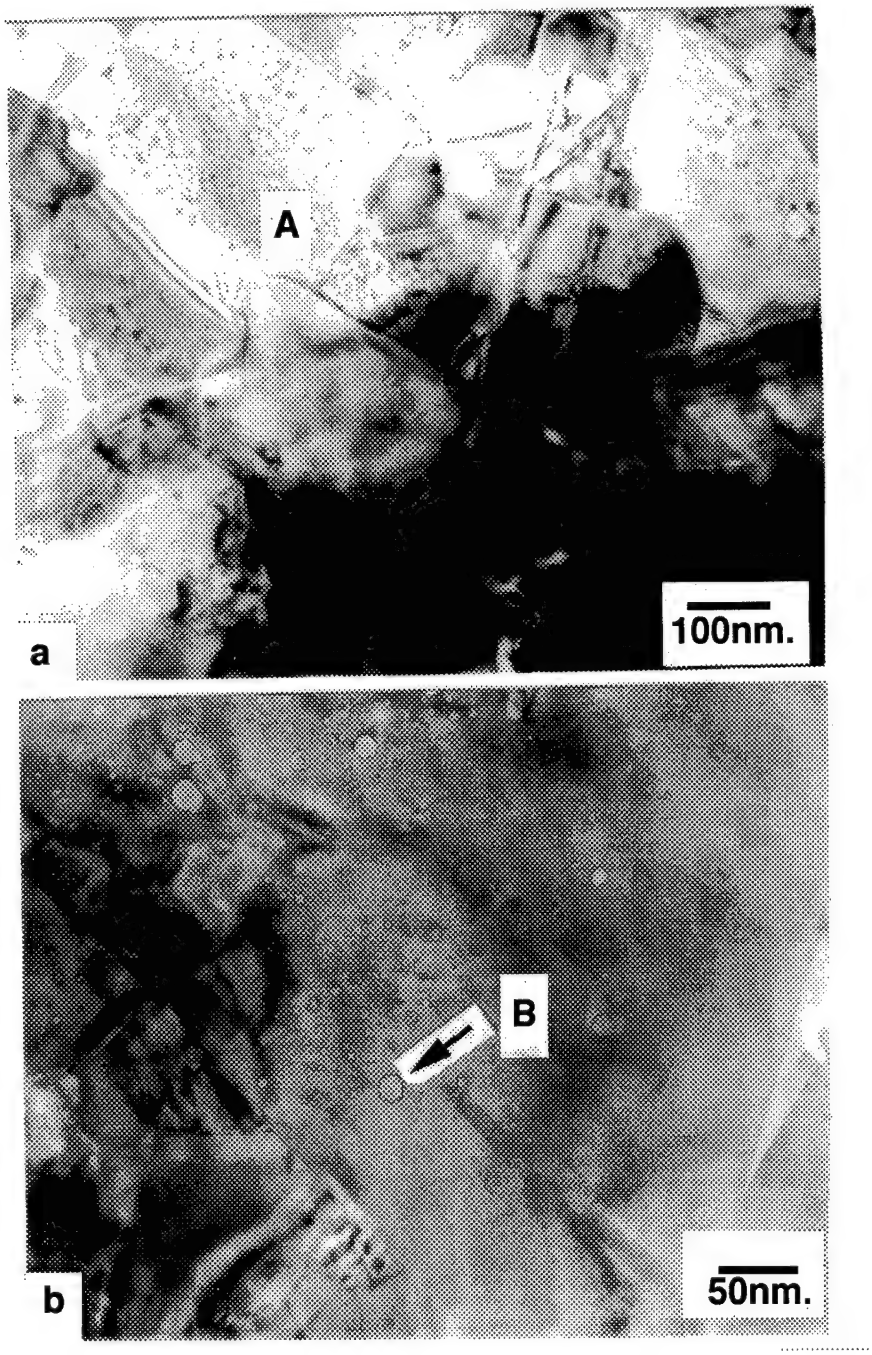

Fig. 9 Electron micrograph of nanostructured WC-6%Co-0.8%VC showing distribution of ultrafine fcc Co precipitates in the WC grains
(a) $[2\bar{1}\bar{1}0]$ zone axis for WC grain A
(b) [0001] zone axis for WC grain B

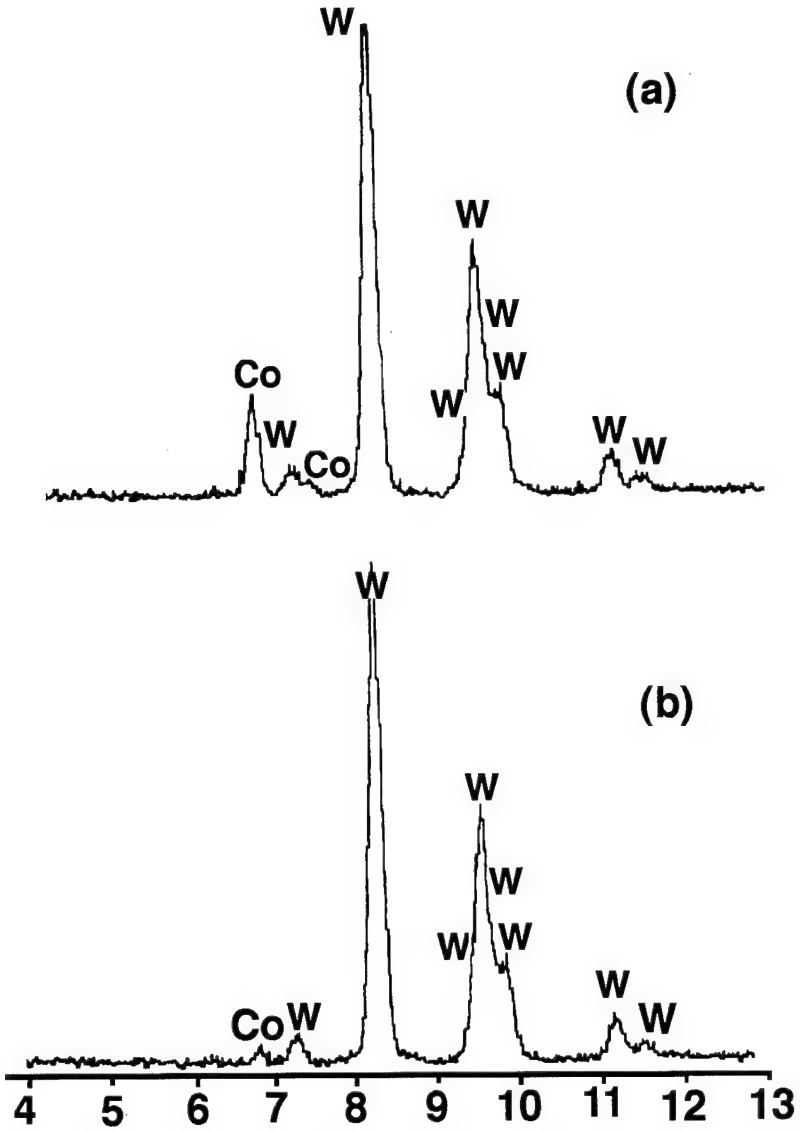

Fig. 10. Analytical electron microscope EDAX spectra for nanostructured WC-6%Co-0.8%VC using a 10nm. probe: (a) a Co precipitate in a WC nanograin, (b) WC nanograin.

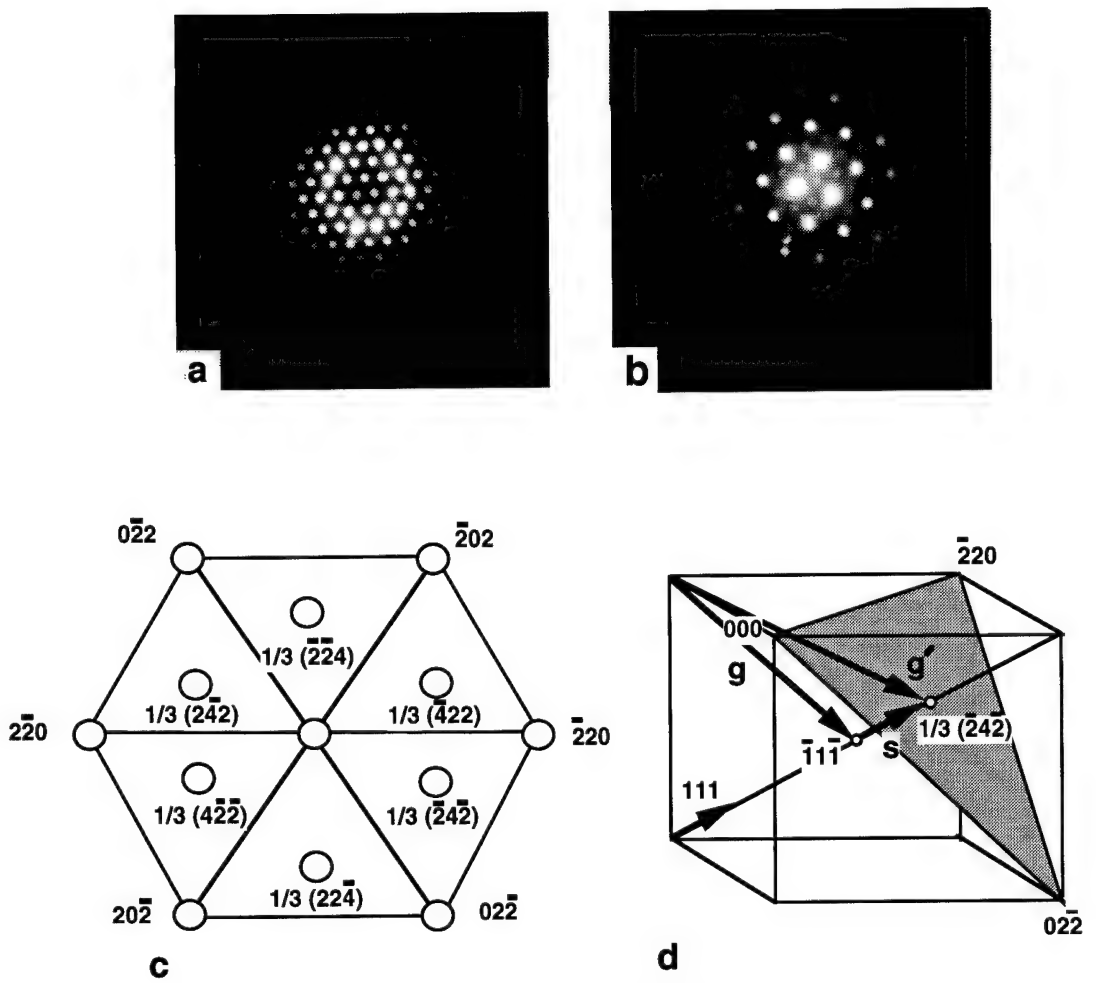

Fig.11 Electron diffraction analysis for nanostructured WC-6%Co-0.8%VC, following 8 hrs. heat treatment at 700°C. Microdiffraction patterns for (a) [0001] zone axis of WC matrix, (b) [111] zone axis of fcc Co nanoprecipitate, (c) analysis of (b) showing primary and satellite reflections, and (d) schematic showing the projection of a <111> type reflection into the zero order Laue zone.

WC-6wt.% Co -VC material consolidated by thermomechanical forming (Ceracon™ process) at 1300°C are seen in Figs.8c.and d. The fact that these materials are of comparable microstructural scale shows that the VC inhibitor is only required in liquid phase sintering because of the rapid grain growth kinetics.

A ubiquitous feature in electron micrographs obtained from all materials listed in Table I is the presence of an ultrafine precipitate phase within the WC nanograins. Examples of these ultrafine precipitates in WC-6wt.%-0.8wt.% VC material are evident in Fig.9a for WC nanograin "A" with a $[2\bar{1}\bar{1}0]$ foil normal and nanograin "B" with a [0001 foil normal. High resolution microscopy shows that the size of these ultrafine precipitate ranges from the limit of resolution to about 20-30 nm. Information on the chemical composition of them was obtained using an analytical electron microscope with a 100Å probe diameter. Comparison of spectra from the adjacent WC matrix and the ultrafine precipitate reveals a particularly high enrichment of cobalt in the ultrafine precipitate, see Figs.10a and b. The crystallographic nature of the ultrafine precipitate phase was determined using the analytical electron microscope in the micro-micro diffraction mode. For reference, Fig.11a shows the [0001] micro-micro diffraction pattern of the hexagonal WC phase. This pattern is used to obtain the camera constant, and hence determine the interplanar spacing of the nanoprecipitate phase. Analysis of diffraction patterns, for different specimen orientations, reveals that the nanoprecipitate has the fcc structure. As an example, Fig.11b shows a [111] pattern with a hexagonal arrangement of strong <220> reflections from the zero order Laue zone; this is shown schematically in Fig.11c. An additional feature in the pattern is the hexagonal arrangement of weaker 1/3<224> reflections, due to intersection of the Ewald sphere with spikes from <111> points in the first Laue zone. The schematic diagram in Fig.11d, shows how, for example, the $\bar{1}1\bar{1}$ reciprocal lattice position is projected along the [111] beam direction to the 1/3 $(\bar{2}4\bar{2})$ position in the zero order Laue zone. Confirmation of the fcc structure was provided by tilting the foil by 20^{o} to obtain the [112] diffraction pattern. Validation that the nanoprecipitates are cobalt is provided by the close agreement between the measured values and values calculated from the standard lattice parameter of $3.544A^{o}$, for fcc cobalt, see Table II. It should be noted that the analysis of the cobalt nanoprecpitates is similar to that employed by R. Ayer, J.Y Koo, J.W. Steeds and B.K.Park in studying ultrafine precipitates in a Al-Mg-Zn-Cu alloy[5].

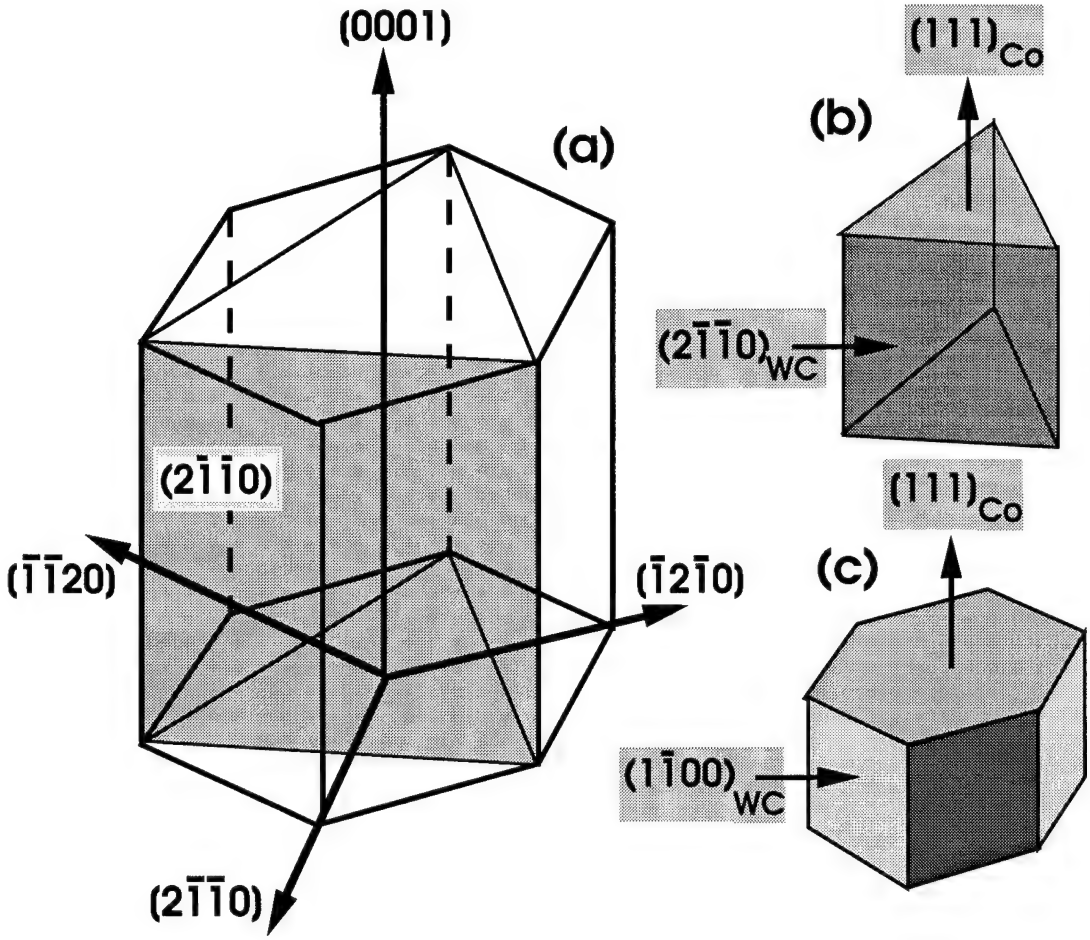

Fig 12. Schematic diagram showing: (a) the Co nanoprecipitate morphology with reference to the hexagonal WC unit cell, (b) and (c) the triangular and hexagonal forms ,as deduced from the electron microscope observations.

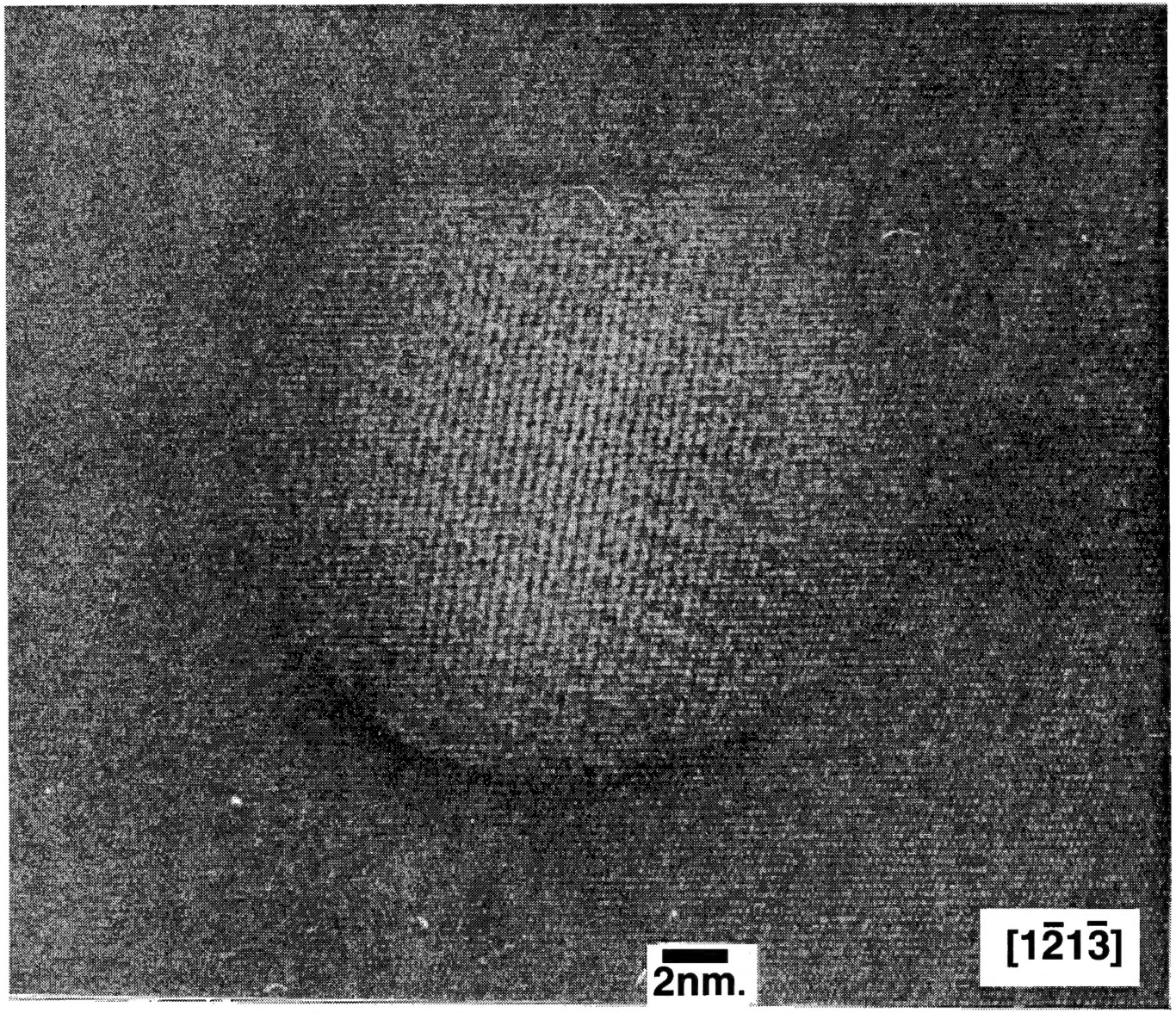

Fig. 13 Atomic resolution image of Co nanoprecipitate in WC nanograin in WC-6wt%Co-0.8%VC material heat treated at 700^{o}C for 8 hours using a high voltage (800kV electrin microscope. The Co nanoprecipitate has undergone modification by preferential etching of Co close to the foil edge.)

TABLE II

Values of the Lattice Parameter		
d spacing	Determined (A^o)	Calculated(A^o)
{220}	1.253	1.27
{311}	1.07	1.07
{111}	2.046	2.05

From the diffraction patterns in Figs. 11a and b for WC-6% Co-0.8% VC material, the [111] zone axis of the cobalt nanoprecipitates is aligned parallel to the [0001] zone of the hexagonal WC matrix. Insight into morphology is gained by from Fig.9. In the view of a WC grain along a [0001] axis (Fig.9a) the precipitates appear hexagonal to triangular in projection, a particularly clear example is the hexagonal precipitate indicated by the arrow. As shown diagrammatically in Fig.12 a hexagonal-form shape in the [0001] projection corresponds to an ultrafine Co-rich precipitate with interfaces parallel to the {1100} planes of the WC matrix phase. Similarly, a triangular-form shape corresponds to an ultrafine Co-rich precipitate with interfaces parallel to the $[2\bar{1}\bar{1}0]$ WC matrix. planes. Also, as is seen from Fig,12 the triangular and hexagonal precipitate prisms project as squares when viewed along the$[2\bar{1}\bar{1}0]$ axis. A dispersion of square-shaped ultrafine precipitates is evident in the$[2\bar{1}\bar{1}0]$ axis WC grain in Fig.9a.

To gain further information on the cobalt nanoprecipitates, images were obtained using the high voltage (800 kV) JEOL ARM-1000 microscope, with atomic resolution capability. A restrictive factor however, was that direct lattice images were only obtainable in thin regions of the foil where cobalt depletion had occurred by preferential etching during specimen preparation. Several regions containing nanoprecipitates, such as that in Fig.6, were observed however. A clear feature in Fig.6[13], is the set of lattice planes with 2.51 Å and 1.87 Å spacing in the WC phase. Continuing work is in progress to investigate the nanoprecipitate images by Fourier transform analysis.

4.3. *Signicance of the Results*

The discovery of Co nanoparticle dispersions within the WC nanograins of WC-Co synthesized from chemical precursors, reflects the efficacy of intimate mixing at the atomic, or molecular level. This shows an inherent difference between elemental mixing, and mechanical blending of particles of the constituent phases (WC and Co), as used in conventional ball-milling. In the initial step of thermochemical processing, the constituent elements are intimately mixed when the precursors are dissolved to form an aqueous solution. Furthermore, chemical homogeneity is maintained throughout the subsequent process steps of spray drying and thermochemical conversion at 700-900°C in a fluid bed reactor. As a result of elemental mixing, some cobalt is retained within nucleated W nanograins, which then transform to WC during the carburization step. The present results show that Co nanopreciptates nucleate from the cobalt retained within the WC nanograins.

It is particularly interesting that Co nanopreciptates were observed in all the consolidated specimens which were examined. This included material consolidated above the eutectic temperature by hot pressing, with and without VC as a grain growth inhibitor. It also included material consolidated below the eutectic temperature by rapid hot working. Consequently, the nucleation of the Co nanopreciptates is not promoted by chemical modification, i.e. the addition of vanadium. A striking feature, however is that Co nanopreciptates are observed in liquid phase sintered material which undergoes substantial coarsening, such that the WC grain diameter becomes as large as 7 microns. This behavior is consistent with the concept that coarsening occurs by the coalescence of WC grains(containing Co nanopreciptates), followed by boundary migration though the coalesced grains. It is certainly inconsistent with the concept of the dissolution of WC nanograins, followed by nucleation and rapid grain growth.

4.3 *References*

1. L. E. McCandlish, B. H. Kear and B. K. Kim, Materials Science and Technology, 1990, **6**, 953

2. B. H. Kear and L. E. McCandlish, "Chemical Processing and Properties of Nanostructured Materials", Nanostructured Materials, 1993, **3**, 19

3. Z. Fang, Rogers Tool Works, private communication, 1994

4. S. Rele, and R. Raman, Ceracon Inc., CA, private communication, 1994

5. R. Ayer, J.Y.Koo, J.W.Steeds and B.K.Parks, "Microanalytical Study of Hetrogeneous Phases in Commercial Al-Mg-Zn-Cu Alloys", Met. Trans. A, 1985, **16a,** No. 11, .1925